Solid State Ionics 28–30 (1988) 886–894
North-Holland, Amsterdam

ELECTROCHEMICAL LITHIUM INTERCALATION IN $Na_{0.33}V_2O_5$ BRONZE PREPARED BY SOL–GEL PROCESSES

J.P. PEREIRA-RAMOS, R. MESSINA
Laboratoire d'Electrochimie, Catalyse et Synthèse Organique, U.M. No. 28, C.N.R.S., 2, rue Henri-Dunant, 94320 Thiais, France

L. ZNAIDI and N. BAFFIER
Laboratoire de Chimie de la Matière Condensée, U.A. 302, C.N.R.S., E.N.S.C.P., 11, rue Pierre et Marie Curie, Paris, France

Received 13 August 1987

Synthesis of monoclinic $Na_{0.33}V_2O_5$ bronze by sol–gel processes and its electrochemical behaviour have been investigated. The four well defined processes evidenced in the potential window 3.5–2 V versus Li/Li^+ are discussed in terms of crystallographic data. The high reversibility of Li^+ ion insertion ($\approx 70\%$ of the initial faradaic yield after the 80th cycle) makes this compound a promising cathodic material for secondary lithium cells.

1. Introduction

Chemical or electrochemical lithium insertion into vanadium pentoxide is known to lead to the formation of lithium vanadium bronzes at ambient temperature [1–4]. Such materials are of interest as positive electrode in ambient temperatures lithium cells [5–8].

In addition to these bronzes, another class of materials which should be of considerable interest for use in lithium cells is the monoclinic β phase of vanadium bronzes, $M_xV_2O_5$ synthesized at high temperature, in which M is an alkali or a transition metal [9]. This structure corresponds to an incorporation of the metal atoms into tunnels of a distorted V_2O_5 lattice. But little has been reported on their evaluation in primary or secondary Li cells. Both electronic and ionic conductivity allow the β-$Li_xV_2O_5$ bronze to be used as a solid solution cathode in high energy secondary batteries [10]. In a more recent electrochemical study, Popov et al. [11,12] have investigated the thermodynamics and kinetics of $Li_xV_2O_5$ bronzes over a wide range of lithium content and temperatures in lithium cells.

The electrochemical conversion of oxygen on the surface of the sodium vanadium oxide bronzes $Na_xV_2O_5$ has been studied in acidic media by Brainina et al. [13]. Very recently, preliminary results reported by Raistrick [14–16] have outlined that $Na_xV_2O_5$ and $K_xV_2O_5$ bronzes are potentially attractive positive electrodes for Li cells.

In order to obtain new interesting cathodic materials, we have attempted to enhance the diffusion of lithium ions into the host lattice of the corresponding vanadium oxide bronze by increasing the initial anisotropy of this structure, the latter obtained by preparing the oxides via the sol–gel process.

The purpose of this work is to discuss the physical and chemical properties of the $Na_{0.33}V_2O_5$ bronze synthesized by the sol–gel process and to present, in relation with the bronze structure, some results about the electrochemical insertion of lithium. The electrochemical study has been carried out in a molten dimethylsulfone-based electrolyte at 150°C, in which a notable improvement of the electrochemical performances for most of the usual cathodic materials has been observed [17,18].

2. The structure of $Na_{0.33}V_2O_5$ bronze

The structure of NaV_6O_{15} bronze has been determined by Wadsley [19] and refined by Kobayashi

0 167-2738/88/$ 03.50

[20]. It is of monoclinic symmetry (space groupe A2/m) and the unit cell which contains two formula units has the dimensions $a=10.08$ Å, $b=3.61$ Å, $c=15.44$ Å, $\beta=109.6°$. The structure consists of zig-zag double strings of VO_6 octahedra forming sheets parallel to the a–c plane. Adjacent sheets are joined by additional chains, parallel to the b axis, of double VO_5 trigonal bipyramids, giving rise to a tunnel structure. Each tunnel in projection contains two interstitial equivalent sites labeled M_1 and M_1' (fig. 1 adapted from refs. [21,22]). The saturation of these sites would give the composition $Na_2V_6O_{15}$ (or $Na_{0.67}V_2O_5$). In the case of $Na_{0.33}V_2O_5$, one can think that the Na^+ ions are distributed equally between the two sites M_1 and M_1', with the appearance of a regular alternation of occupied and vacant sites. Furthermore, Galy et al. [21] have shown that this bronze structure presents two other possible tunnel sites: an eight-coordinated site M_2 and a tetrahedral site M_3. All tunnel sites are of the same symmetry: 4i Wyckoff position of the monoclinic space group.

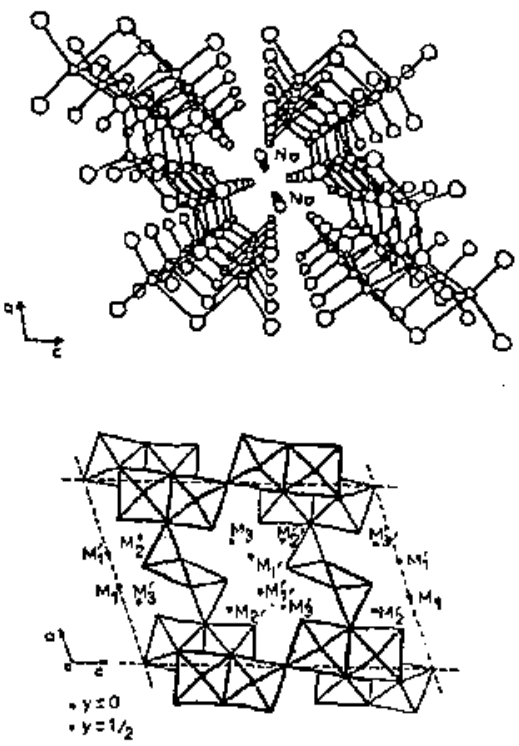

Fig. 1. Crystal structure of β-$Na_{0.33}V_2O_5$ and possible positions of the inserted cations (adapted from refs. [21,22]).

Thus, this compound has a highly anisotropic structure and can lead, in the case of NaV_6O_{15} monocrystal, to quasi-one-dimensional properties for electrical conductivity: conductivity of the semiconductor type along the b-axis exceeding by two orders of magnitude from that in the a–c plane [23].

3. Experimental procedures

3.1. Synthesis of the $Na_{0.33}V_2O_5$ bronze via sol-gel process

The basic material is V_2O_5 gels with formula $V_2O_5 \cdot nH_2O$ prepared by polycondensation of vanadic acid. The latter is obtained by an ion-exchange technique: a metavanadate solution is allowed to pass through a bed of resin (Dowex 50WX$_2$, 50–100 mesh). Most of the water contained in V_2O_5 gel readily evaporates at room temperature leading to a xerogel $V_2O_5 \cdot 1.6H_2O$. It is formed of entangled fibers which are ribbon-shaped with dimensions $10 \times 10^2 \times 10^3$ Å^3 [24]. If the xerogel is deposited as layer onto a glass plate, its X-ray diffraction pattern in reflection geometry is that typical of a layered structure resulting from the parallel arrangement of the ribbons on the substrate. The basic distance is $d=11.5$ Å [25] (fig. 2a). Thus, in this way, the anisotropic structure of the orthorhombic V_2O_5 is highly enhanced. This material behaves as a layered host structure and can intercalate easily a large variety of ionic species, just by dipping the sample in an aqueous solution of the corresponding chloride [26]. The sodium xerogel which is obtained in the case of a total reaction [27] has the formula $Na_{0.33}V_2O_5 \cdot 1.6H_2O$ and corresponds to a layer spacing of 10.9 Å (fig. 2b). This compound gives rise to the $Na_{0.33}V_2O_5$ bronze after evaporation of the water molecules at moderate temperature (350°C).

3.2. Electrochemical measurements

3.2.1. Electrolytes

Dimethylsulfone ($DMSO_2$) was obtained from Janssen. $DMSO_2$ (m.p.: 109°C) was first recrystallized in water and then twice from absolute methanol, air dried at 90°C for 48 h and then sublimated under reduced pressure (2 mm Hg) at 100°C. It was

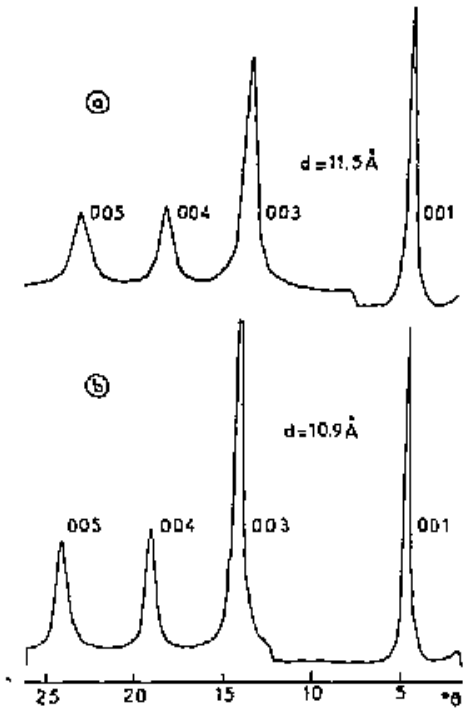

Fig. 2. X-ray diffraction patterns (Co Kα) from $V_2O_5 \cdot 1.6\ H_2O$ (a) and $Na_{0.33}V_2O_5 \cdot 1.6\ H_2O$ (b) in reflection geometry.

then conserved in an argon glove box. Under these conditions, the water concentration did not exceed 5×10^{-3} mol kg^{-1}. Anhydrous lithium perchlorate (Fluka) was dried under vacuum at 200°C for 12 h. The electrolytes were prepared under a purified argon atmosphere.

3.2.2. Experimental technique

The working electrode consisted of either a nickel, or a gold, or a stainless-steel grid 1 cm in diameter, on which a finely ground powder of the β-$Na_{0.33}V_2O_5$ bronze, mixed with graphite (90% by weight) or without graphite, was pressed. Such a treatment did not give rise to a loss of anisotropy of the starting sodium bronze. Lithium was used as reference electrode and aluminium as counterelectrode. The electrochemical cell has already been described [17]. It was thermostated with silicone oil, whose temperature (±1°C) and circulation were controlled by a Huber T200 thermostat.

The X-ray analysis of the electrochemically formed bronzes $Li_xNa_{0.33}V_2O_5$ was performed on samples pressed on a nickel or a gold grid without graphite, with a CGR (Theta60) X-ray system using Co $K\alpha_1$ radiation (λ=0.1789 nm). Before analysing, the electrodes were washed under an argon flow with dried and degassed distilled tetrahydrofuran (THF) and then dried under vacuum at ambient temperature.

4. Results and discussion

4.1. Characterization of the β bronze obtained by the sol–gel process (SGP bronze)

Thermal analysis results of the sodium xerogel (DTA and GTA curves) are shown in fig. 3. The two endothermic peaks observed on the DTA curve at 120 and 300°C correspond to the elimination of weakly bonded and more strongly bonded water molecules respectively. The thermogram indicates two weight losses of about 1.3 H_2O and 0.3H_2O respectively. Finally, the exothermic peak at 320°C corresponds to the crystallization of the bronze.

In order to compare this bronze obtained by the sol–gel process (SGP bronze) and the usual bronze obtained through solid state reactions at 650°C (SSR bronze), X-ray diffraction experiments have been performed in reflection geometry for the two compounds (fig. 4). The two bronzes are monoclinic and the parameters of the SGP bronze (a=10.10±0.05 Å, b=3.63±0.01 Å, c=15.45±0.05 Å, β=110.0 ±0.5°C) are close to those of the SSR bronze. But

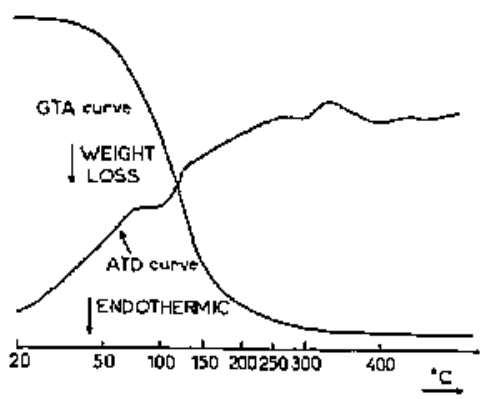

Fig. 3. DTA and TGA curves from $Na_{0.33}V_2O_5 \cdot 1.6\ H_2O$.

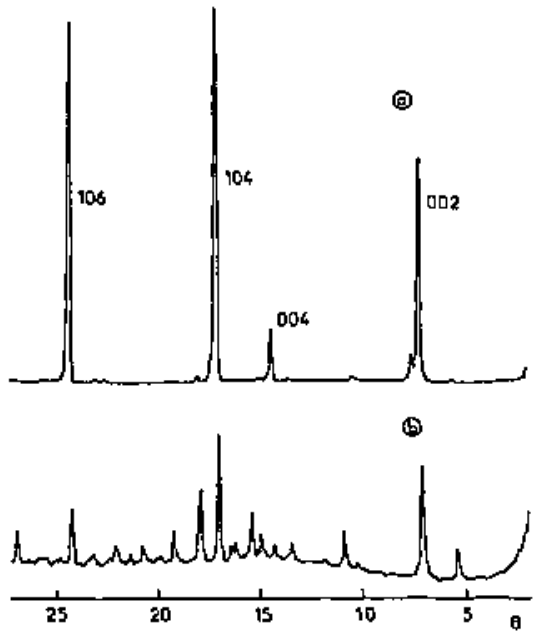

Fig. 4. X-ray diffraction patterns (Co Kα) from $Na_{0.33}V_2O_5$ bronzes in reflection geometry: SGP bronze (a) and SSR bronze (b).

Table 1
X-ray diffraction intensity data in reflection geometry (Co Kα) for SGP bronze and for SSR bronze of the same formula $Na_{0.33}V_2O_5$

$h\,k\,l$	I/I_0	
	SGP	SSR
1 0 0	0.4	25
0 0 2	45	90
1 0 2	0.2	5
2 0 0	0.1	30
1 0 $\bar{4}$	0.2	10
0 0 4	10	10
2 0 2	0	20
1 1 $\bar{1}$	0.1	37
1 1 1	0	10
1 0 4	100	100
3 0 $\bar{4}$	0.5	55
2 1 1	0	25
4 0 $\bar{2}$	0	12
3 1 $\bar{1}$	0	6
4 0 0	0	15
3 1 1	0	8
1 0 6	70	45
5 0 $\bar{4}$	0	27

the intensities of peaks are considerably different (table 1): only the Bragg peaks 002, 004, 104 and 106 correspond to noticeable intensities for the SGP bronze. Of course, the other Bragg peaks can be observed on a transmission pattern. So diffraction patterns reveal preferred orientation corresponding to an alignment of the tunnels over larger domains parallel to the *a–b* plane. Thus, it is clear that the anisotropy of the structure is very enhanced by the preparation via sol–gel process.

In the same way, electrical conductivity of the SGP bronze is highly anisotropic, giving vlaues of $\sigma_{\parallel} \approx 2\ \Omega^{-1}\ cm^{-1}$, and $\sigma_{\perp} \approx 2 \times 10^{-3}\ \Omega^{-1}\ cm^{-1}$ at room temperature.

4.2. Electrochemical lithium insertion in SGP bronze

4.2.1. Electroanalytical measurements and relation with structural properties

Typical chronopotentiometric curves for the reduction and oxidation at constant current of $Na_{0.33}V_2O_5$ in 1 mol kg^{-1} $LiClO_4/DMSO_2$ are shown in fig. 5. Four well shaped reduction processes are observed in the potential range 3.5–2 V, which correspond to the electrochemical insertion of lithium into the sodium vanadium bronze according to

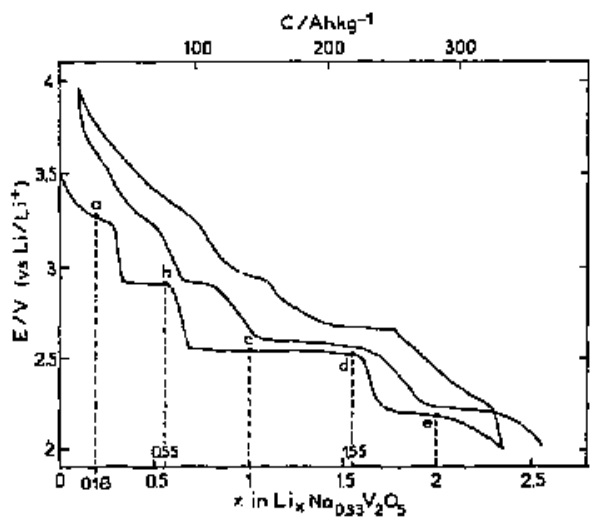

Fig. 5. Cyclic chronopotentiograms performed at constant current (400 μA/cm^2) for a $Na_{0.33}V_2O_5$ electrode in 1 mol kg^{-1} $LiClO_4$ solution in molten $DMSO_2$ at 150°C.

$$Na_{0.33}V_2O_5 + xe^- + xLi^+ \rightleftharpoons Li_xNa_{0.33}V_2O_5 ,$$

with $x_{max} \approx 2.5$.

The different steps are separated by sharp voltage changes. Up to about $x \approx 0.3$, the voltage and hence the chemical potential of lithium changes continuously from 3.5 to 2.9 V. On the other hand, the second, and the third step appear as voltage plateaux at 2.9 and 2.55 V for lithium contents corresponding to $0.3 < x < 0.7$ and $0.7 < x < 1.7$ respectively. These results are in good agreement with the EMF data reported by Raistrick at ambient temperature [15]. However, the last reduction process occurring at 2.2 V for a lithium content $1.7 < x < 2.5$ has never been reported as yet.

Utilization of current densities in the range 0.1–1 mA/cm^2 gives rise to a negligible polarization with a still practically identical Faradaic yield ($x = 2.3/2.5$), which shows that $Na_{0.33}V_2O_5$ exhibits a high electronic conductivity and also that lithium is highly

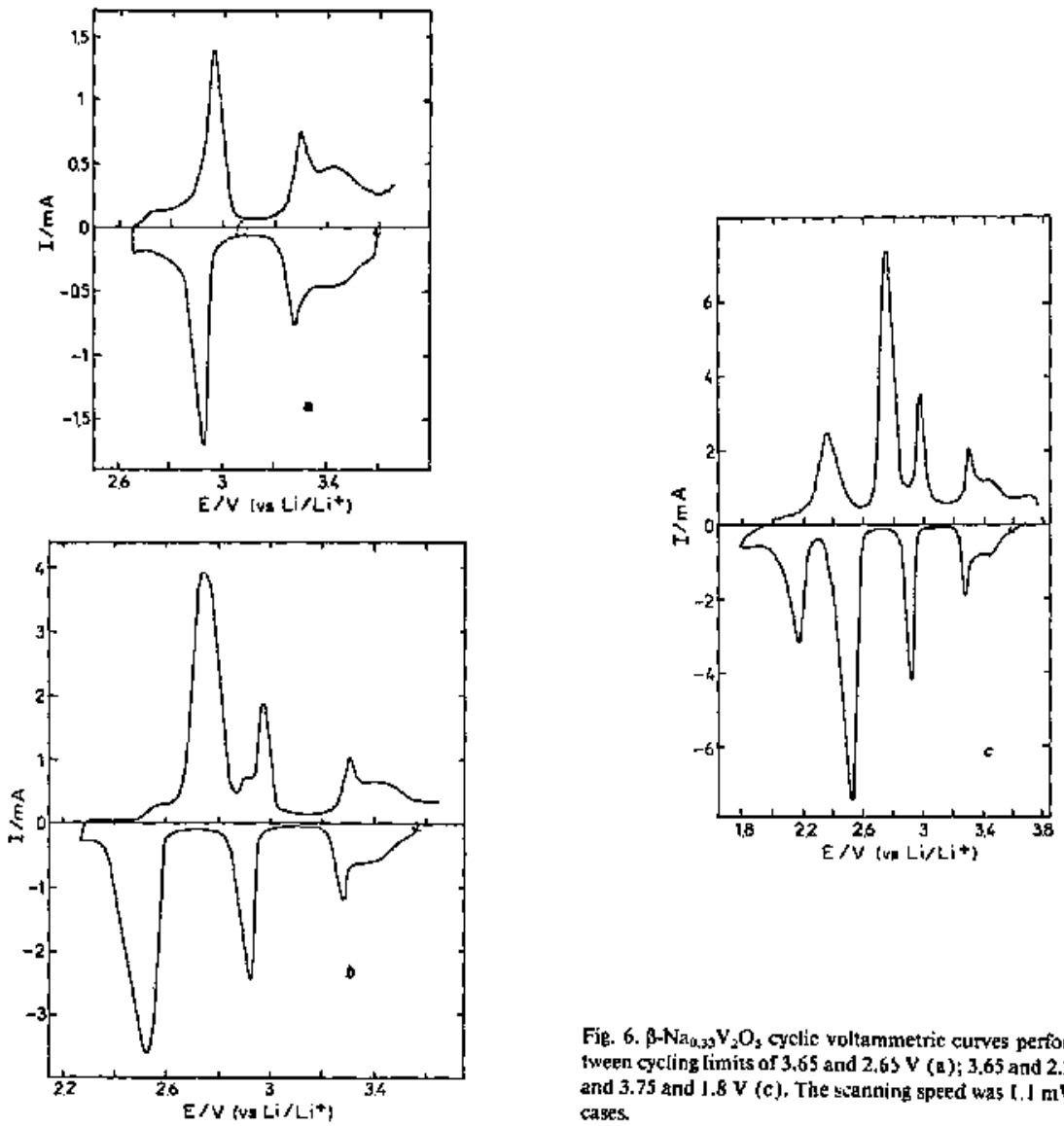

Fig. 6. β-$Na_{0.33}V_2O_5$ cyclic voltammetric curves performed between cycling limits of 3.65 and 2.65 V (a); 3.65 and 2.25 V (b) and 3.75 and 1.8 V (c). The scanning speed was 0.1 mV/s in all cases.

mobile in the electroformed bronzes.

Reversibility of each insertion process has been evaluated from a cyclic voltammetric study (fig. 6). For all the steps examined, the voltammetric curves exhibit very well defined cathodic and anodic peaks. The difference ΔE_p between the anodic and cathodic peaks varies with the cutoff voltage of the cathodic scanning. For the first two steps, we have $\Delta E_p \approx 20$ and 40 mV, whereas $\Delta E_p \approx 200$ mV for the last two processes. This indicates that electrochemical lithium insertion into the sodium vanadium bronze is more reversible for $0 < x < 0.7$ than for higher lithium contents. But even after cathodic scanning has been performed after the last reduction process, a satisfactory reversibility is found as indicated in fig. 6. However, in all cases, the amount of electricity required for the reduction and recovered in the oxidation is practically similar. Such quantitative data have been confirmed by galvanostatic measurements (fig. 5).

The observed potential discontinuities in the chronopotentiometric curves and the very high reversibility of the insertion have suggested to correlate these results with the structural properties of the SGP bronze. X-ray diffraction patterns in reflection geometry have been made for different values of the lithium content situated between the potential steps (see table 2). They show that the monoclinic β structure is stable at least up to $x = 1.6$, which corresponds to two alkali ions per V_2O_5 ($M_2V_2O_5$), i.e. 12 alkali ions per unit cell ($M_{12}V_{12}O_{30}$). According to Pouchard [28], the parameters listed in table 2 show that only the c parameter varies perceptibly with composition, although the domain of composition is much more important in this present study. This very important result confirms the hypothesis or the observations made by some authors [3,4,11,14] that the chemical or electrochemical lithium incorporation at RT in orthorhombic V_2O_5 or in monoclinic β bronze does not change the basic network, apart from inducing a few variations in one or two parameters.

Table 2
Structural parameters for various Li contents in $Li_xNa_{0.33}V_2O_5$

x	Total alkali metal content	a (Å)	b (Å)	c (Å)	β (deg)
0.0	0.33	10.10	3.63	15.45	110.0
0.18	0.51	10.17	3.62	15.34	110.0
0.60	0.93	10.12	3.63	15.15	110.0
1.0	1.33	10.08	3.64	15.10	110.0
1.6	1.93	10.11	3.72	15.09	110.0
2.0	2.33	9.7	3.74	15.10	110.0

Table 3
Separation M–M for the three different sites of the tunnel structure of the β-$M_xV_2O_5$ bronze

Sites	d (Å)
M_1M_1'	2.22
M_2M_1	2.84
M_3M_1'	4.14
M_1M_1''	2.12
M_2M_3'	1.90

One can thus try to correlate the potential steps to the partial occupancy of the different tunnel sites of the structure. The steps have been found for ≈4, 6 and 12 alkali ions per unit cell. According to the same 4-multiplicity of the sites and to their easier half-occupancy, one can suggest that the occupancy is easier the larger is the distance between an already occupied site and a vacant site. The distances listed in table 3 show that the first step and the second step occurring for total alkali contents of 0.63 and 1 could correspond to half-occupancy of the M_3 sites (between 3.5 and 2.9 V) and of the M_2 sites (at ≈2.9 V) respectively. Then, by convenience of symmetry, when the three sites are all half-occupied, there is no reason for a potential step during the gradual occupancy of the three equivalent sites to appear, i.e. up to $x = 1.7$. However, the total occupancy of the three sites would correspond to a smaller separation of the nearest-neighbour sites (about 2 Å) and could explain the lower reversibility of the insertion after the two first steps.

Beyond $x = 1.7$, it is not sure whether the β structure remains stable. Although the reversibility of the Li insertion is still good (fig. 6c), we shall see that this result is not confirmed during the cycling behaviour.

We have tried to oxidize a fresh sample of $Na_{0.33}V_2O_5$ at a low constant current up to the theoretical amount of electrons, corresponding to the complete removal of sodium. After this procedure, a discharge curve identical to that obtained on a fresh

sample has been obtained. It can be concluded that sodium is very stable in the β-$Na_{0.33}V_2O_5$ structure. In this respect, Steele [29] was also unable to change the sodium composition of $Na_{0.33}V_2O_5$ by coulometric titration in the temperature range 100–450°C. On the contrary, a RMN [30] and an electrochemical study [11] of high temperature β-$Li_xV_2O_5$ have proved a lithium mobility, even at ambient temperature. Such a feature is very interesting for the application of the β-$Na_{0.33}V_2O_5$ bronze as reversible cathodic material, since control of the upper voltage limit is not a factor which affects the rechargeability of the sodium bronze.

4.2.2. Cycling behaviour

Regarding the high capacity exhibited by the cathodic material (up to 2.5 $Li^+/Na_{0.33}V_2O_5$) and the interesting reversibility evidenced in both galvanostatic and voltammetric measurements, we have evaluated the cycling behaviour of $Na_{0.33}V_2O_5$ within cycling limits of 3.8 and 1.8 V at a current density of 1 mA/cm².

The specific capacity recovered during cycling falls dramatically from its initial value of 300 Ah kg^{-1} up to about 50 Ah kg^{-1} by the 70th cycle, i.e. to a capacity of 20% of the initial one (fig. 7). On the other hand, when cycling experiments are performed in the

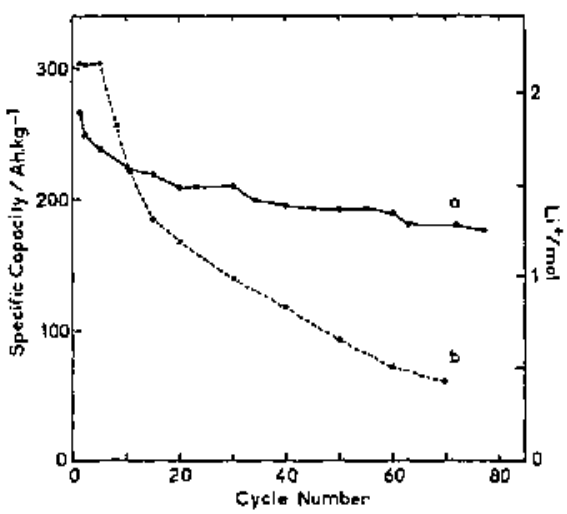

Fig. 7. Cathode utilization versus cycle number for the extended cycling of the β-$Na_{0.33}V_2O_5$ bronze (1 mA/cm²) in the potential window 3.8–2.24 V (a) and 3.8–1.8 V (b).

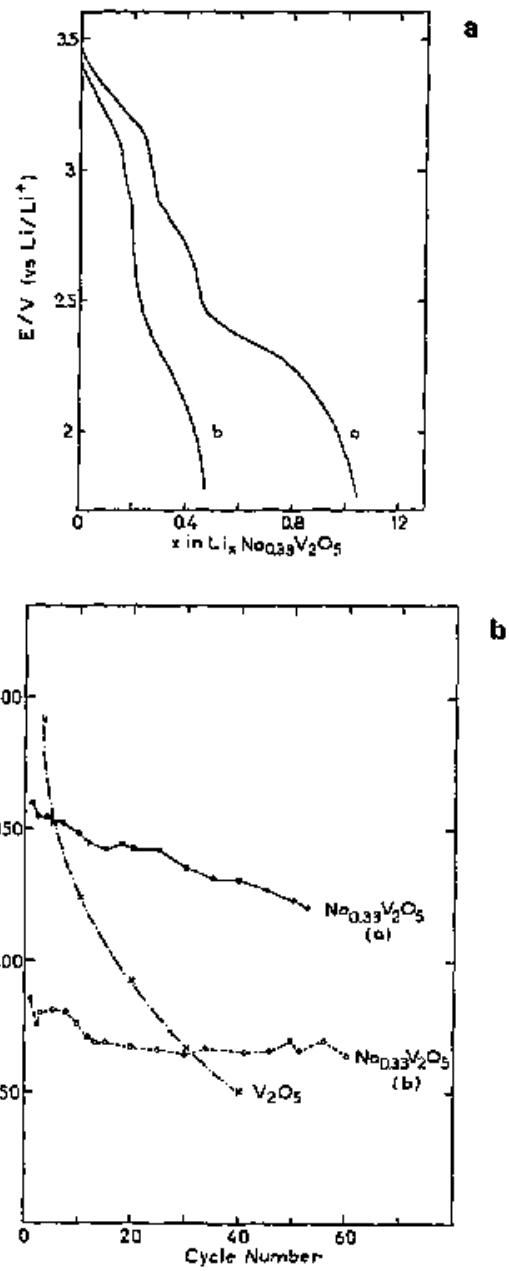

Fig. 8. (a) Comparison of the discharge curves obtained for the SGP bronze (a) and the SSR bronze (b) at room temperature (1 mA/cm², 1 M $LiClO_4$/PC). (b) Cathode utilization versus cycle number for the SGP (a) and SSR (b) bronzes, and the orthorhombic vanadium pentoxide V_2O_5 tested in 1 M $LiClO_4$/PC electrolyte at room temperature (1 mA/cm², cycling limits 3.8 and 1.8 V).

potential window 3.8–2.24 V, i.e. up to a lithium content of $x \approx 1.7$, a satisfactory behaviour is observed. Indeed, after the 80th cycle, about 180 A h kg^{-1}, i.e. 70% of the initial capacity, is recovered. As we have seen above, this influence of the depth of discharge on the cycling behaviour can be correlated with the structural data obtained from X-ray analysis: the cycling behaviour is satisfactory up to the total occupancy of the three equivalent sites, while it becomes deficient beyond $x \approx 1.7$ Li per $Na_{0.33}V_2O_5$.

Control of the lower voltage limit of cycling appears to be of utmost importance to avoid irreversible reduction of the β-$Na_{0.33}V_2O_5$.

An extension of the evaluation of $Na_{0.33}V_2O_5$ cathodes to Li cells has been made at ambient temperature with the 1 M $LiClO_4$/propylene carbonate as organic electrolyte. Fig. 8 shows a plot of cathode utilization versus cycle number for the SGP bronze, for a SSR bronze of the same composition and for orthorhombic V_2O_5. One can see that the SGP bronze gives rise to the highest capacity during extensive cycling experiments. Thus, the sol–gel technique allows preparation of a bronze in which the diffusion of lithium ions is made easier by aligning the tunnels over larger domains along their common direction.

5. Conclusion

Four well defined processes for the electrochemical insertion of lithium ions into the SGP β-$Na_{0.33}V_2O_5$ bronze have been evidenced. Taking the separation of sites M–M in the tunnel structure of β-$Na_{0.33}V_2O_5$ and the X-ray experiments into account, the first two steps have been correlated with the half-occupancy of sites M_3 and M_2 respectively, while the third is ascribed to the filling of the three different sites. Up to $x \approx 1.7$, about 70% of the initial capacity obtained at 150°C in molten $DMSO_2$, i.e. 180 Ah kg^{-1}, is recovered whereas beyond $x \approx 1.7$ the cycling behaviour of the SGP bronze is rather poor. From extended cycling experiments performed at room temperature, the β-$Na_{0.33}V_2O_5$ synthesized by the sol–gel technique appears to be a very promising cathodic material for reversible Li batteries, even as compared to other vanadium oxides such as V_6O_{13} and $Li_{1+x}V_3O_8$ [31].

Acknowledgement

The financial support by the Direction des Recherches, Etudes et Techniques (D.R.E.T., Decision no. 871157) is gratefully acknowledged.

References

[1] M.S. Whiningham and M.B. Dines, J. Electrochem. Soc. 124 (1977) 1387.
[2] M.S. Whittingham, J. Electrochem. Soc. 122 (1975) 713; 123 (1976) 315.
[3] P.G. Dikens, S.J. French, A.T. Hight and M.F. Pye, Mater. Res. Bull. 14 (1979) 1295.
[4] D.W. Murphy, P.A. Christian, F.J. Di Salvo and J.V. Waszczak, Inorg. Chem. 18 (1979) 2800.
[5] C.R. Walk and J.S. Gore, J. Electrochem. Soc. 122 (1975) 686.
[6] A. Tranchant, R. Messina and J. Perichon, J. Electroanal. Chem. 113 (1980) 225.
[7] N. Kumagai and K. Tanno, Denki Kagaku 48 (1980) 432.
[8] N. Kumagai and K. Tanno, Electrochim. Acta 28 (1983) 17.
[9] P. Hagenmuller, in: Non-stoichiometric compounds, tungsten bronzes, vanadium bronzes and related compounds, Vol. 1, eds. D.J. Bevan and P. Hagenmuller (Pergamon Press, Oxford, 1973) p. 569.
[10] W.L. Roth and G.C. Farrington, U.S. Patent No. 3, 970, 473 (1976).
[11] A.V. Popov, Yu.G. Metlin and Yu.D. Tretyakov, J. Solid State Chem. 32 (1980) 343.
[12] Yu.D. Tretyakov, A.V. Popov and Yu.G. Metlin, Solid State Ionics 17 (1985) 265.
[13] Kh.Z. Brainina, E.V. Bazarova and V.L. Volkov, Elektrokhimiya 16 (1980) 69, 1203.
[14] I.D. Raistrick and R.A. Huggins, Mater. Res. Bull. 18 (1983) 337.
[15] I.D. Raistrick, Solid State Ionics 9/10 (1983) 425.
[16] I.D. Raistrick, Rev. Chim. Minér. 21 (1984) 456.
[17] J.P. Pereira-Ramos, R. Messina and J. Perichon, J. Power Sources 16 (1985) 193.
[18] J.P. Pereira-Ramos, R. Messina and J. Perichon, J. Appl. Electrochem. 16 (1986) 379.
[19] A.D. Wadsley, Acta Cryst. 8 (1955) 695.
[20] H. Kobayashi, Bull. Chem. Soc. Japan 52 (1979) 1315.
[21] J. Galy, J. Darriet, A. Casalot and J.B. Goodenough, J. Solid State Chem. 1 (1970) 339.
[22] T. Erata, J. Chem. Soc. Japan 36 (1981) 297.
[23] R.H. Wallis, N. Sol and A. Zylbersztein, Solid State Commun. 23 (1977) 539.
[24] J.J. Legendre and J. Livage, J. Colloid Interface Sci. 94 (1983) 75.
[25] P. Aldebert, N. Baffier, N. Gharbi and J. Livage, Mater. Res. Bull. 16 (1981) 669.

[26] A. Bouhaouss, P. Aldebert, N. Baffier and J. Livage, Rev. Chim. Minér. 22 (1985) 17.
[27] L. Znaidi, D. Lemordant and N. Baffier, Solid State Ionics, to be published.
[28] M. Pouchard, Thesis, Bordeaux University (1967).
[29] B.C.H. Steele, in: Mass transport phenomena in ceramics, eds. A.R. Cooper and A.H. Heuer (Plenum Press, New York, 1975) p. 269.
[30] J. Gendell, R.M. Cotts and M.J. Sienko, J. Chem. Phys. 37 (1962) 220.
[31] M. Pasquali, G. Pistoia, V. Manev and R.V. Moshtev, J. Electrochem. Soc. 133 (1986) 2454.